Voltage Source Multilevel Inverter Voltage Quality Comparison under Multicarrier Sinusoidal PWM and Space Vector PWM of Two Delta Voltages

Nikolay N. Lopatkin
Mathematics, physics and informatics department
Shukshin Altai State Humanities Pedagogical University (ASHPU)
Biysk, Russia
nikolay_lopatkin@mail.ru

***Abstract*—The three-phase multilevel inverter output voltage waveforms are compared for the recently proposed simple voltage source multilevel inverter space vector PWM technique, which uses the natural nonsymmetric three-segment vectors switching sequence, and for the traditionally applied in industry multicarrier sinusoidal PWM, namely the phase opposition disposition (POD) PWM. The two variants of the POD sinusoidal PWM technique with the opposite carriers phases are considered. The developed waveforms mathematical models were implemented in LabVIEW virtual instruments for simulation. The values of the total harmonic distortion (THD), the first order integral voltage harmonics factor and the zero and first orders indices of the so-called aggregate switchings and integrated voltage harmonics factors are presented as the functions of the amplitude modulation index for the five lowest values of the frequency modulation index. The simulation results have proved the clear superiority of the offered space vector PWM technique in the aggregate indices values.**

Keywords*—pulse width modulation inverters; space vector pulse width modulation; total harmonic distortion; multilevel voltage source inverter; sinusoidal PWM (SPWM); level-shifted multicarrier modulation; phase opposition disposition PWM (POD PWM); space vector PWM of two delta voltages; n-order integral voltage harmonics factor; n-order aggregate switchings and integrated voltage harmonics factor

I. INTRODUCTION

The present-day stage of the PWM technique evolution in power electronics area is characterized by the active phase of the space vector PWM (SVPWM) application to the multilevel voltage source inverters (MLVSI) [1, 2]. The advantages combining of the above mentioned control method and the circuitry is now available due to the readiness of various SVPWM techniques for the high effective implementation by cheap microprocessors, DSP or FPGA. This is also the basis for further development and refinement of the modulation method for various MLVSI topologies.

While the SVPWM has well known advantages in comparison with the carrier-based PWM, like the better input direct voltage source usage and the better inverter output capability, there are trends towards not only the results convergence of these two techniques using but also their joint (combined) use [3]. In fact, the study of sinusoidal PWM (SPWM) models and refinement of their characteristics for the increased MLVSI levels number still continue [4-7].

II. PROBLEM DEFINITION

The simple SVPWM technique for the quarter-wave symmetric output voltage waveform formation of the three-phase multilevel inverter with arbitrary levels number, based on the applying the appropriate natural nonsymmetric three-segment vectors switching sequence to the simple voltage source multilevel inverter space vector PWM algorithm [8-11], has been recently proposed [12-14]. The accurate mathematical description of the offered technique is provided by [14]. Nevertheless, in addition to [12, 13], comparisons with existing and widely spread in industry PWM techniques are needed.

The most frequently implemented PWM schemes are the phase-shifted and the level-shifted multicarrier modulations [15, 16]. And the simplest of them is the multicarrier SPWM existing in some different kinds.

Probably, the most popular and easily implemented kind of the multicarrier SPWM is the phase opposition disposition (POD). In the POD, the positive and negative carriers are in phase, but between them, there is the 180 degrees phase shift [15, 16, 4-6].

There are two variants of the POD, having 0 and 180 degrees phase delay of the positive carrier triangular waves, respectively. They are called here POD-0 and POD-180 and shown in Fig. 1 a) and b), correspondingly.

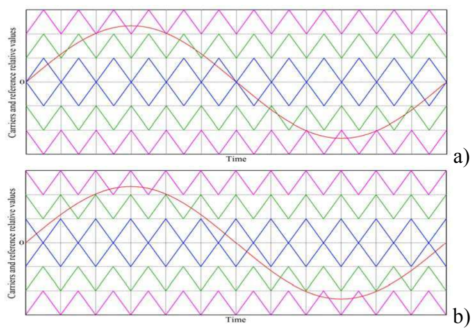

Fig. 1. Carriers and reference waveforms of the phase opposition disposition method: a) POD-0 with 0 degrees phase delay of the positive carriers; b) POD-180 with 180 degrees phase delay of the positive carriers.

The purpose of this paper is to compare the three-phase MLVSI output voltage waveforms of the two above mentioned POD variants and the simple SVPWM algorithm of two delta voltages under the proposed three-segment vectors switching sequence [12-14]. This comparison has been performed by the total harmonic distortion (THD), the first order integral voltage harmonics factor (IHF) [17] and the zero and first orders aggregate switchings and integrated voltage harmonics factors (ASIHF) [13] values for the five lowest values of the frequency modulation index to research modes with low switching loses values. Thus, here just main coefficients, related to the load current quality and to the price of voltage quality achieving (in form of the rising of the switches commutation frequency), has been considered.

III. Mathematical Models

Herein after voltages marked with an asterisk (*) are the relative values, in relation to the input DC voltage of the unit level U_d.

The basical delta voltage waveform formation principle of the recently offered SVPWM algorithm of two delta voltages [14] is as follows:

$$u^*_{kEXExy}(t_c) = \lfloor u^*_{ksREFxy} \rfloor + f_{kEXExy}(t_c)\,, \tag{1}$$

here $u^*_{kEXExy}(t_c)$ is the relative value of the instantaneous output delta voltage u_{xy} that is being executed during the current time t_c from the start of the clock cycle with number k, $k = 1 \dots m_f$, m_f is the frequency modulation index, $m_f = f_c / f$, f_c and f are, respectively, clock and modulating frequencies;

$u^*_{ksREFxy}$ is the relative value of the instantaneous reference delta voltage u_{REFxy} sampled for the midpoint of the k-th clock cycle;

$\lfloor w \rfloor$ means the rounding down w to the closest integer number, taking into account the sign (the "floor" function);

$f_{kEXExy}(t_c)$ is the function, which is being executed during the clock cycle with number k, and it can possess only the values 0 and 1; the clock cycle mean value $\bar{f}_{kEXExy}$ of this function should correspond to the fractional part of the relative value of the instantaneous reference delta voltage u_{REFxy} :

$$\bar{f}_{kEXExy} = \{ u^*_{ksREFxy} \}, \tag{2}$$

$\{w\}$ means the fractional part of w.

In this paper, unlike [14], the reference delta voltage amplitude is $\sqrt{3} \cdot m_a$, since the amplitude modulation index m_a is defined as follows:

$$m_a = U / U_d = U^*, \tag{3}$$

here U and U^* are the value and the relative value of the voltage space vector magnitude, equal to the reference phase voltage amplitude.

The phase x executed phase-to-ground voltage $u^*_{\mathrm{EXE}xg}$ for POD level-shifted multicarrier modulation can be expressed in form:

$$u^*_{\mathrm{EXE}xg} = \left(\left\lfloor \left| u^*_{REFx} \right| \right\rfloor + \frac{1}{2} \left(\mathrm{sgn}\left(\left\{ \left| u^*_{REFx} \right| \right\} - u^*_{carr} \right) + 1 \right) \right) \times$$
$$\times \mathrm{sgn}\left(u^*_{REFx} \right), \tag{4}$$

here u^*_{REFx} is the relative value of the reference instantaneous phase voltage u_{REFx} (here the sinusoidal one);

u^*_{carr} is the only carrier signal (here the triangular one) with the peak-to-peak amplitude equal to the unite;

$$\mathrm{sgn}(w) = \begin{cases} -1 & if\ w < 0 \\ 0 & if\ w = 0 \\ 1 & if\ w > 0. \end{cases}$$

Since the load is assumed to be balanced, the phase-to-neutral executed voltages can be derived from phase-to-ground voltages for POD and from delta voltages for SVPWM:

$$\begin{bmatrix} u^*_{EXEan} \\ u^*_{EXEbn} \\ u^*_{EXEcn} \end{bmatrix} = \frac{1}{3} \cdot \begin{bmatrix} 2 & -1 & -1 \\ -1 & 2 & -1 \\ -1 & -1 & 2 \end{bmatrix} \cdot \begin{bmatrix} u^*_{EXEag} \\ u^*_{EXEbg} \\ u^*_{EXEcg} \end{bmatrix} = \frac{1}{3} \cdot \begin{bmatrix} 2 & 1 \\ -1 & 1 \\ -1 & -2 \end{bmatrix} \cdot \begin{bmatrix} u^*_{EXEab} \\ u^*_{EXEbc} \end{bmatrix}. \tag{5}$$

Due to some advantages in comparison to PSIM and to our existing groundwork [18, 19], the graphical programming environment LabVIEW was chosen for the simulations.

The waveforms of the reference absolute value integer and fractional parts for POD are shown in Fig. 2. The resulted voltages waveforms for POD-0, POD-180 and SVPWM under the mode with $m_f = 36$, $m_a = 3.4$ are shown in Fig. 3. The reference node of the phase-to-ground voltages (the ground) is the MLVSI neutral node.

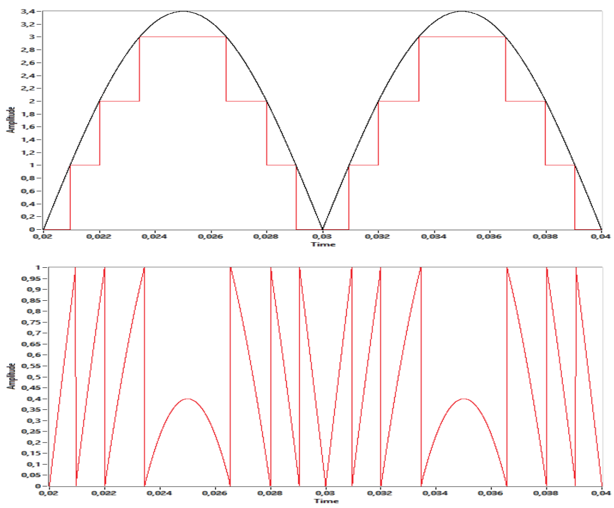

a)

b)

Fig. 2. LabVIEW-simulated POD reference signal for $m_a = 3.4$: a) the absolute value (black curve) and its integer part (red curve); b) the fractional part of the absolute value.

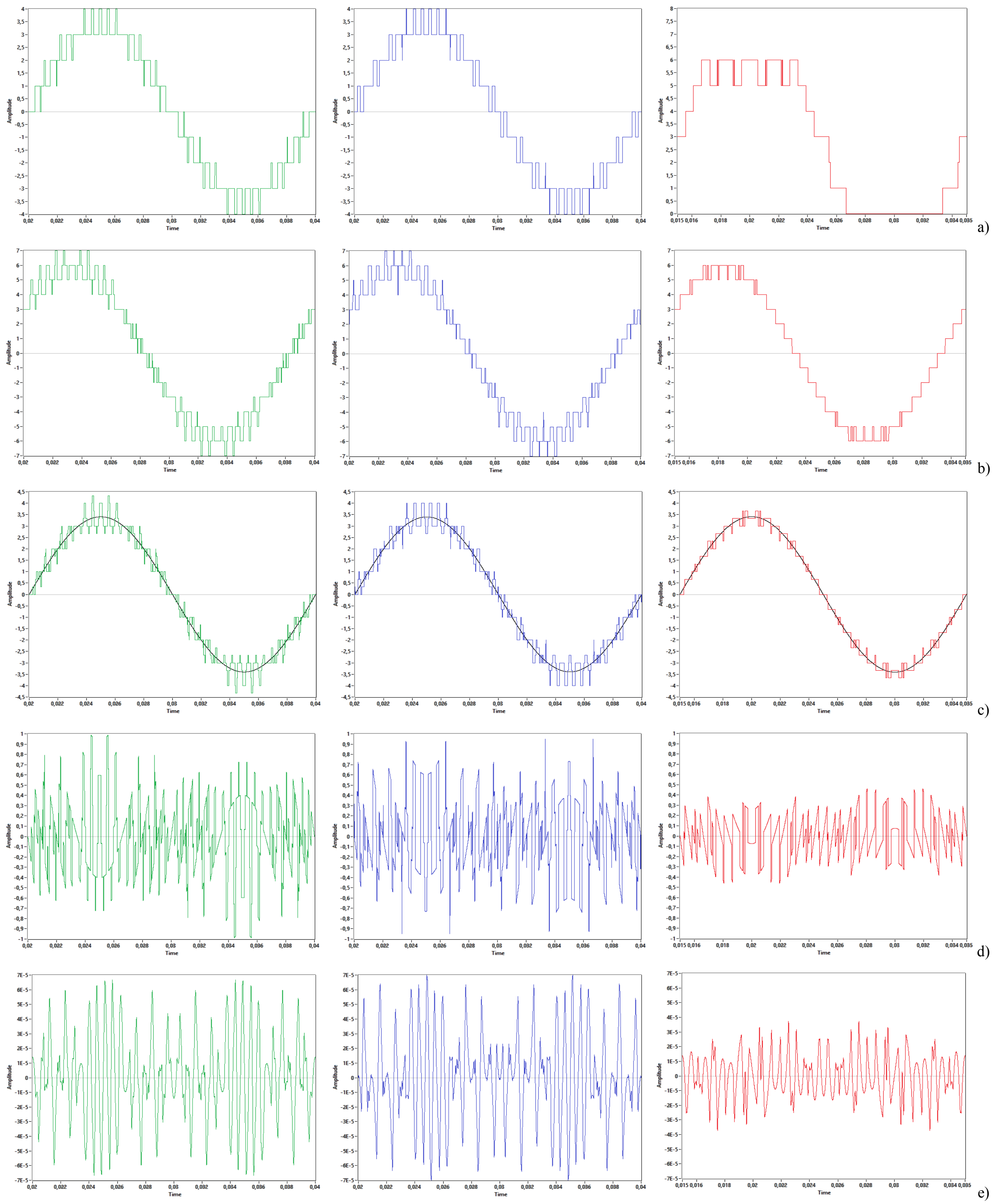

Fig. 3. LabVIEW-simulated output voltages idealized waveforms for the POD-0 (green curves), the POD-180 (blue curves) and the offered SVPWM technique (red curves) under $m_f = 36$, $m_a = 3.4$: a) the phase-to-ground voltages; b) the delta voltages; c) the phase-to-neutral voltages and their fundamental components; d) the high harmonics components of the phase-to-neutral voltages; e) the integrated high harmonics components of the phase-to-neutral voltages.

IV. Harmonics Factors Simulation Results

A. THD and First Order Integral Voltage Harmonics Factor

The first order integral voltage harmonics factor (IHF) $\overline{K}_{hu}^{(1)}$ [17, 20, 18, 19], also called weighted THD (WTHD) factor [15], provides the estimate of relative harmonics content in a researched signal after the action of the idealized first order integrating electric circuit:

$$\overline{K}_{hu}^{(1)} = \frac{\overline{U}_{(hh)}^{(1)}}{\overline{U}_{(1)}^{(1)}} = \frac{\overline{U}_{(hh)}^{(1)} \cdot \omega}{U_{(1)}}, \qquad (6)$$

here $U_{(1)}$, $\overline{U}_{(1)}^{(1)}$ and $\overline{U}_{(hh)}^{(1)}$ are the RMS value of the voltage fundamental component and RMS values of the results of the single indefinite integral taking of the instantaneous values of the fundamental component $\overline{u}_{(1)}^{(1)}$ and of the high harmonics component $\overline{u}_{(hh)}^{(1)}$ (see Fig. 3 e)) of the whole voltage, correspondingly; ω is the angular frequency of the fundamental component.

In many cases, one can estimate the output current THD of some ohmic-inductive loaded inverter as proportional to corresponding voltage first order IHF [17, 20].

The phase-to-neutral voltage THD and the first order IHF simulated curves for the considered POD and SVPWM variants as the functions of the amplitude modulation index (up to 6) under the frequency modulation index values 12, 18, 24, 30 and 36 are shown in Fig. 4 and Fig. 5.

B. Switchings Number and Aggregate Switchings and Integrated Voltage Harmonics Factors

The number of the switchings in the MLVSI phase leg (the number of the phase-to-ground voltage relative value changings by 1) per the output voltage cycle N_{swph} is used here as the generic value for different MLVSI circuits for the MLVSI power switches dynamical losses preliminary assessment.

The used here so-called *n*-order aggregate switchings and integrated voltage harmonics factor (ASIHF) [13] is defined as follows:

$$\overline{K}_{hu-aggr-sw}^{(n)} = N_{swph} \cdot \overline{K}_{hu}^{(n)}, \qquad (7)$$

here $\overline{K}_{hu}^{(n)}$ is the *n*-order IHF, $n = 0$ and $n = 1$ correspond to the THD and the first order IHF (see (6)), respectively.

Such the aggregate indices, taking into account both the voltage harmonics and the number of the switchings, were first proposed in [20, 21]. The *n*-order normalized integral (weighted) harmonic factor in [22] is coincident to (7) just for $n = 1$, i.e. for the first order ASIHF $\overline{K}_{hu-aggr-sw}^{(1)}$ [13].

The phase-to-neutral voltage zero and first order ASIHF simulated dependences on the amplitude modulation index (up to 6) for the considered POD and SVPWM PWM variants under the frequency modulation index values 12, 18, 24, 30 and 36 are presented in Fig. 6.

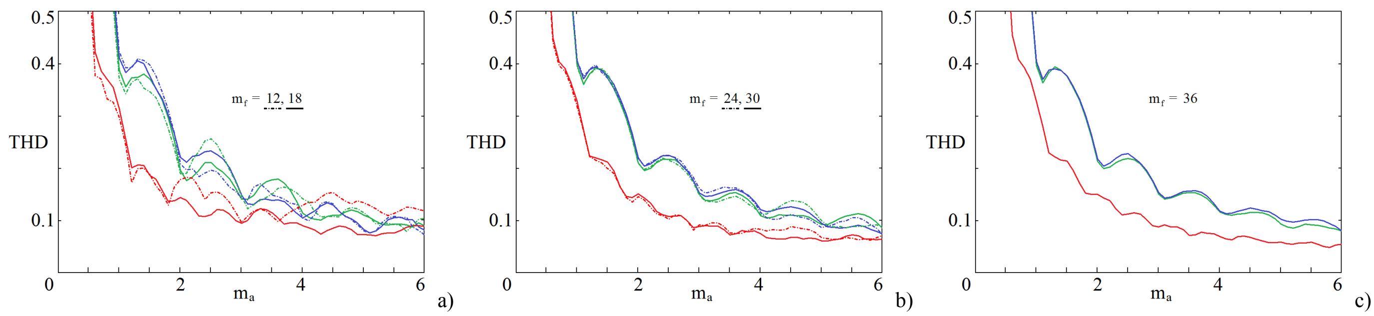

Fig. 4. LabVIEW-simulated dependences of the MLVSI phase-to-neutral voltage THD on the amplitude modulation index for the POD-0 (green curves), the POD-180 (blue curves) and the offered SVPWM technique (red curves) under the different low values of the frequency modulation index: a) $m_f = 12$ and $m_f = 18$; b) $m_f = 24$ and $m_f = 30$; c) $m_f = 36$.

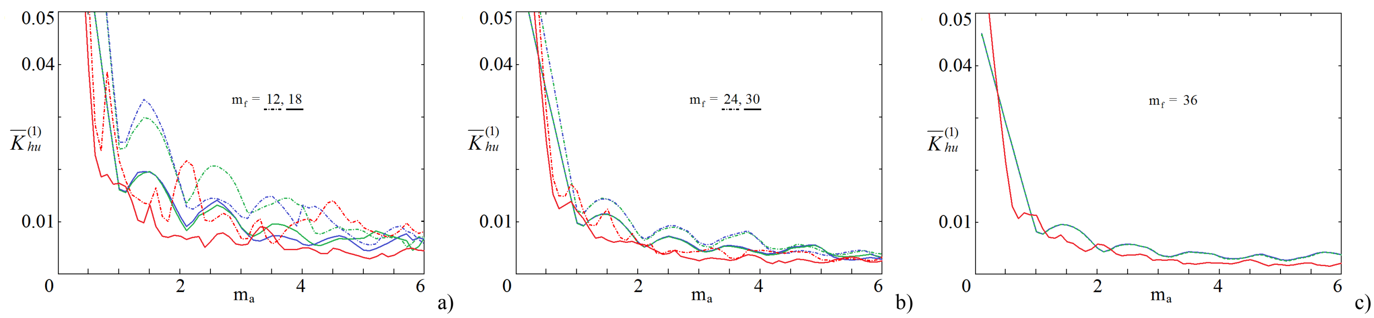

Fig. 5. LabVIEW-simulated dependences of the MLVSI phase-to-neutral voltage first order integral voltage harmonics factor on the amplitude modulation index for the POD-0 (green curves), the POD-180 (blue curves) and the offered SVPWM technique (red curves) under the different low values of the frequency modulation index: a) $m_f = 12$ and $m_f = 18$; b) $m_f = 24$ and $m_f = 30$; c) $m_f = 36$.

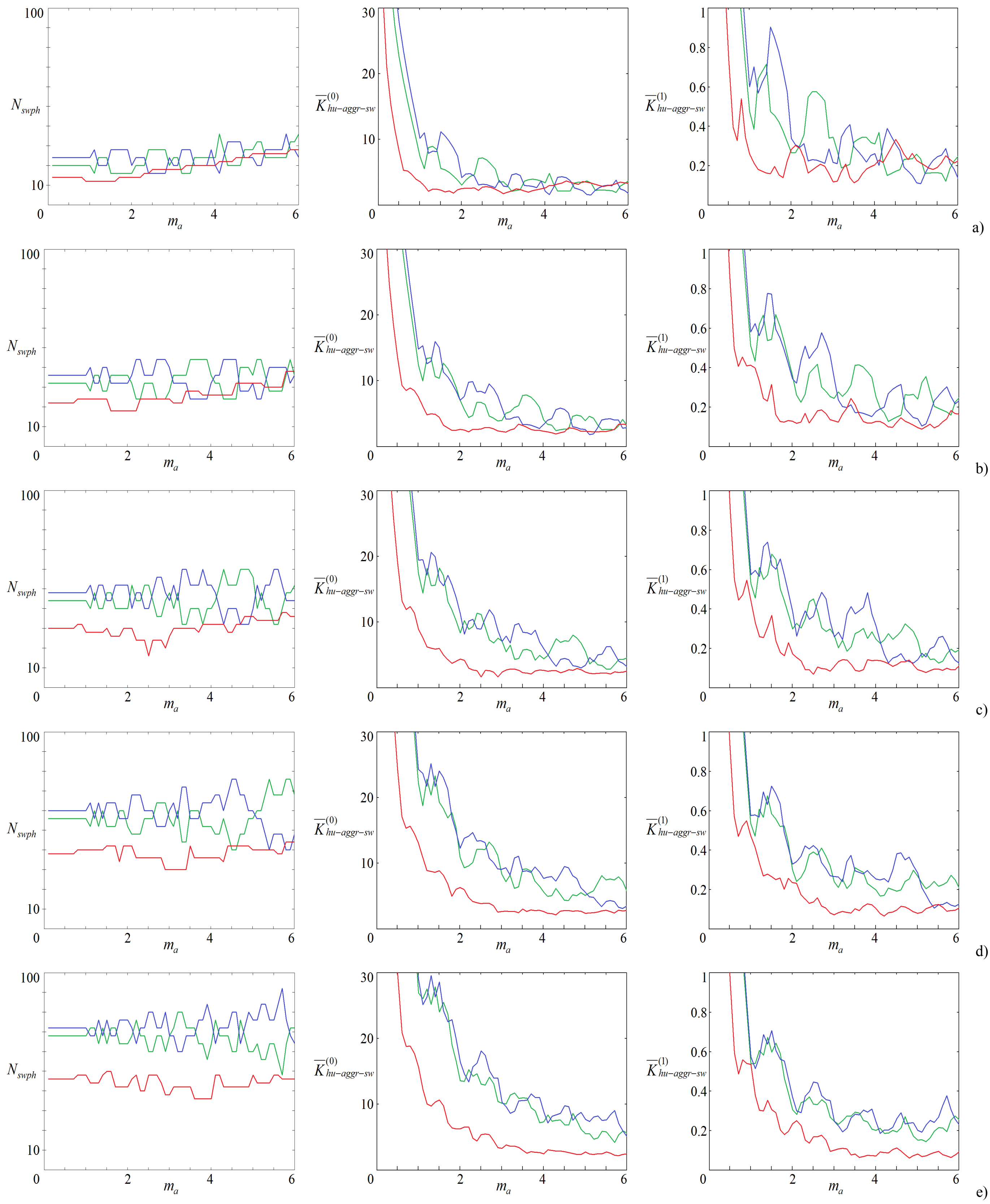

Fig. 6. LabVIEW-simulated dependences of the MLVSI phase leg switchings numbers, the zero order aggregate switchings and integrated voltage harmonics factor and the first order aggregate switchings and integrated voltage harmonics factor of the phase-to-neutral voltage on the amplitude modulation index for the POD-0 (green curves), the POD-180 (blue curves) and the offered SVPWM technique (red curves) under the different values of the frequency modulation index: a) $m_f = 12$; b) $m_f = 18$; c) $m_f = 24$; d) $m_f = 30$; e) $m_f = 36$.

As can be seen from Fig. 4 and Fig. 5, the more the frequency modulation index is, the less difference between the two POD variants in the both THD and the first order IHF values is. The POD modulating technique is competitive with the offered SVPWM technique at the only lowest value of the frequency modulation index ($m_f = 12$): beginning from the amplitude modulation index value of about 4 all the considered indicators (the THD, the first order IHF, the zero and the first order ASIHF, see Fig. 4…Fig. 6) have the less values for the POD sinusoidal PWM.

In the rest of cases all of the offered SVPWM technique results turned out to be better. The particularly compelling evidence of this SVPWM scheme advantage is the values of the aggregate switchings and integrated voltage harmonics factors (see Fig. 6) which contain data on the total impact of the voltage quality degree and the price of its achieving.

V. Conclusion

The three-phase multilevel inverter output voltage waveforms are compared for the recently proposed simple voltage source multilevel inverter space vector PWM technique, having the natural three-segment vectors switching sequence, and for the traditionally applied in industry multicarrier sinusoidal phase opposition disposition PWM. The values of the THD, the first order integral voltage harmonics factor and the zero and first orders indices of the aggregate switchings and integrated voltage harmonics factors are presented as the LabVIEW-simulated functions of the amplitude modulation index for the five lowest values of the frequency modulation index. The clear superiority of the offered space vector PWM technique in the aggregate indices values have been proved.

References

[1] J.I. Leon, S. Kouro, J. Rodriguez, Bin Wu, "The essential role and the continuous evolution of modulation techniques for voltage-source inverters in the past, present, and future power electronics," IEEE Transactions on Industrial Electronics, Vol. 63, Iss. 5, May 2016, pp. 2688-2701.

[2] I.A. Bakhovtsev, G.S. Zinovev, "PWM methods evolution," APEIE-2016, 13th International Conference on Actual Problems of Electronic Instrument Engineering (APEIE – 39281), Novosibirsk, October 3-6, 2016. Proceedings, Vol. 10, pp. 129-144. (in Russian).

[3] Yao Wenxi, Hu Haibing, Lu Zhengyu, "Comparisons of space-vector modulation and carrier-based modulation of multilevel inverter," IEEE Transactions on Power Electronics, vol. 23, iss. 1, pp. 45-51, January 2008.

[4] G.S. Konstantinou, V.G. Agelidis, "Performance evaluation of half-bridge cascaded multilevel converters operated with multicarrier sinusoidal PWM techniques," ICIEA 2009, 4th IEEE Conference on Industrial Electronics and Applications (ICIEA), China, Xi'an, May 25-27, 2009. Proceedings, pp. 3399-3404.

[5] S.N. Adithya, R.S. Raghu, "Study of multilevel sinusoidal PWM methods for cascaded H-bridge multilevel inverters," 2014 IEEE 2nd International Conference on Electrical Energy Systems (ICEES), India, Chennai, January 7-9, 2014. Proceedings, pp. 249-254.

[6] Ranjan, D.V. Bhaskar, N. Parida, "Analysis and simulation of cascaded H-bridge multi level inverter using level-shift PWM technique," Proceedings of 2015 International Conference on Circuit, Power and Computing Technologies (ICCPCT), India, Nagercoil, March 19-20, 2015.

[7] J. Sabarad, G.H. Kulkarni, "Comparative analysis of SVPWM and SPWM techniques for multilevel inverter," 2015 International Conference on Power and Advanced Control Engineering (ICPACE), India, Bangalore, August 12-14, 2015. Proceedings, pp. 232-237.

[8] N.N. Lopatkin, "Some new representations of the multilevel inverter voltage space vector in the complex plane," SIBCON-2015, 2015 International Siberian Conference on Control and Communications (SIBCON), Russia, Omsk, May 21-23, 2015. Proceedings, IEEE Catalog Number: CFP15794-CDR. ISBN: 978-1-4799-7102-2, 222em.pdf.

[9] N.N. Lopatkin, "Simple delta voltages space vector PWM algorithm for voltage source multilevel inverters," 2016 2-nd International Conference on Intelligent Energy and Power Systems (IEPS), Ukraine, Kyiv, June 7-11, 2016. Conference Proceedings, IEEE Catalog Number: CFP1605X-PRT. ISBN: 978-1-5090-1767-6, pp. 149-154.

[10] N.N. Lopatkin, "Output voltage simulation of multilevel inverter with space vector modulation of two delta voltages," Tekhnichna Elektrodynamika (Technical Electrodynamics), Institute of Electrodynamics NAS of Ukraine, Kyiv, Iss. 5, 2016, pp. 20-22. (In Russian).

[11] N.N. Lopatkin, "Voltage harmonics integral factors estimation of multilevel inverter with space vector modulation of two delta voltages," APEIE-2016, 13th International Conference on Actual Problems of Electronic Instrument Engineering (APEIE – 39281), Novosibirsk, 3-6 October, 2016. Proceedings, Vol. 1, part 3, pp. 112-115.

[12] N.N. Lopatkin, "Voltage quality comparison of space vector PWM voltage source multilevel inverter under symmetric and nonsymmetric switching sequence variants: voltage waveforms, spectra and THD," ICIEAM-2017, 2017 3rd International Conference on Industrial Engineering, Applications and Manufacturing (ICIEAM). IEEE Conference # 40534. Peter the Great Saint-Petersburg Polytechnic University. Russia, St. Petersburg, May 16-19, 2017. Proceedings. Paper 3.4.58 (pp. 1-8), in press.

[13] N.N. Lopatkin, G.S. Zinoviev, "Voltage quality comparison of space vector PWM voltage source multilevel inverter under symmetric and nonsymmetric switching sequence variants: voltage harmonics integral factors," ICIEAM-2017, 2017 3rd International Conference on Industrial Engineering, Applications and Manufacturing (ICIEAM). IEEE Conference # 40534. Peter the Great Saint-Petersburg Polytechnic University. Russia, St. Petersburg, May 16-19, 2017. Proceedings. Paper 3.4.59 (pp. 1-7), in press.

[14] N.N. Lopatkin, "Simple space vector PWM scheme with quarter-wave symmetric output voltage waveform for three-phase multilevel inverter," 2017 International Multi-Conference on Engineering, Computer and Information Sciences (SIBIRCON). Technopark of Novosibirsk Akademgorodok (Academpark), September 18-24, 2017. Proceedings. PID4934551.pdf (pp. 1-6), in press.

[15] D.G. Holms, T.A. Lipo, Pulse Width Modulation for Power Converters. Piscataway, NJ: IEEE Press, 2003.

[16] Bin Wu, M. Narimani, High-Power Converters and AC Drives. Second Edition. Wiley-IEEE Press, 2017.

[17] G.S. Zinoviev, Power Electronics. Textbook for undergraduate students. Fifth edition. Moscow: Jurajt, 2012. 667 p. (in Russian).

[18] N.N. Lopatkin, Y.A. Chernov, "Virtual instrument for nonconventional total harmonic distortion factors evaluation," SIBCON-2016, 2016 International Siberian Conference on Control and Communications (SIBCON), Russia, Moscow, May 12-14, 2016. Proceedings, Moscow, National Research University "Higher School of Economics", IEEE Catalog Number: CFP16794-CDR. Online ISSN: 2380-6516, 166ni7n.pdf.

[19] N.N. Lopatkin, Y.A. Chernov, "Differential and integral factors of harmonics LabVIEW estimation," EDM'2016, 17th International Conference of Young Specialists on Micro/Nanotechnologies and Electron Devices (EDM), Erlagol, Altai, 30 June - 4 July, 2016. Proceedings, pp. 493-498.

[20] G.S. Zinovyev, Direct Methods of Calculation of Power Indicators of Valve Converters. Novosibirsk: NSU, 1990. 220 p. (in Russian).

[21] I.A. Bakhovtsev, G.S. Zinoviev, "Energy conversion quality analysis of PWM autonomous voltage inverter," Power thyristor converters, Interuniversity collection of scientific papers, edition of Novosibirsk Institute of Electrical Engineering (NETI), Novosibirsk, 1987, 162 p. Edited by G.V. Grabovetskiy, pp. 3-12. (in Russian).

[22] I.A. Bakhovtsev, G.S. Zinoviev, "Generalized analysis of output power of multiphase multilevel PWM voltage source inverters," Electricity, Iss. 4, 2016, pp. 26-33. (in Russian).